Spatially Constrained Organic Diquat Anolyte for Stable Aqueous Flow Batteries

Jinhua Huang,[†,‡,§] Zheng Yang,[†,¶,§] Vijayakumar Murugesan,[†,¶] Eric Walter,[¶] Aaron Hollas,[¶] Baofei Pan,[†,‡] Rajeev S. Assary,[†,‡] Ilya A. Shkrob,[†,‡] Xiaoliang Wei,[†,¶,#] Zhengcheng Zhang[†,‡,]**

[†] Joint Center for Energy Storage Research (JCESR)

[‡] Argonne National Laboratory, 9700 Cass Ave., Lemont, IL 60439, USA

[¶] Pacific Northwest National Laboratory, 902 Battelle Blvd., Richland, WA 99352, USA

[#] Present Address: Indiana University-Purdue University Indianapolis (IUPUI), 723 W. Michigan St., Indianapolis, IN 46202, USA

AUTHOR INFORMATION

Corresponding Authors

* Email: xwei18@iupui.edu (X.W.)

* Email: zzhang@anl.gov (Z. Z.)

Author Contributions

§ J. H. and Z. Y. contributed equally to this work.

This is the author's manuscript of the article published in final edited form as:

Huang, J., Yang, Z., Murugesan, V., Walter, E., Hollas, A., Pan, B., … Zhang, Z. (2018). Spatially Constrained Organic Diquat Anolyte for Stable Aqueous Flow Batteries. ACS Energy Letters, 3(10), 2533–2538. https://doi.org/10.1021/acsenergylett.8b01550

ABSTRACT: Redox-active organic materials (ROMs) are becoming increasingly attractive for use in redox flow batteries as promising alternatives to traditional inorganic counterparts. However, the reported ROMs are often accompanied by challenges, including poor solubility and stability. Herein, we demonstrate that the commonly used diquat herbicides, with solubilities of >2 M in aqueous electrolytes, can be used as stable anolyte materials in organic flow batteries. When coupled with a ferrocene-derived catholyte, the flow cells with the diquat anolyte demonstrate long galvanic cycling with high capacity retention. Notably, the mechanistic underpinnings of this remarkable stability are attributed to the improved π-conjugation originated from the near-planar molecular conformations of the spatially constrained 2,2'-bipyridyl rings, suggesting a viable structural engineering strategy for designing stable organic materials.

TOC GRAPHICS

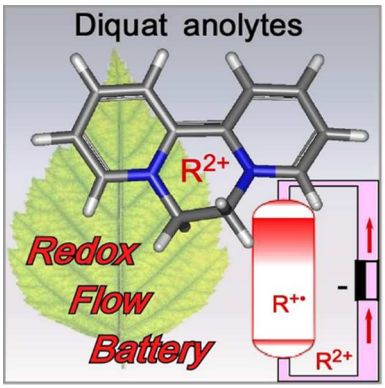

Large-scale electric energy storage systems will be needed to enable reliable integration of intermittent renewable sources such as solar or wind, as well as to improve the stability and efficiency of the current power infrastructure, for smart grid applications.[1-2] Redox flow batteries (RFBs) are among the most attractive electrochemical approaches to this goal. Based on liquid solutions of energized redox-active materials stored in external tanks, RFBs decouple the energy and power, thus allowing independent scalability and flexible designs for different grid applications. Traditional RFBs (such as all-vanadium and zinc-bromine systems) utilize inorganic species, but their use is restricted due to their limited energy density, expensive component materials, narrow redox-active material choices, and/or inferior long-term cyclability.[3-6] Redox-active organic materials (ROMs) have the potential to address the above challenges of inorganic materials, and also have the advantages of being more structurally pliable and compatible with both aqueous and nonaqueous electrolytes.[7-8] While nonaqueous systems generally suffer from the high electrolyte resistivity, ROM-based aqueous RFBs have demonstrated encouraging physico-chemical properties and performance parameters.[9-11] Since the pioneering work on quinoid materials,[12-14] aqueous soluble derivatives of nitroxide radicals,[15] metallocenes,[16] and heterocyclic aromatic compounds[17-21] have been investigated as ROMs for such cells. However, very few of these ROMs have met the materials requirements for achieving energy-dense, long-cycle RFBs and most of them suffer from limited solubility, low chemical stability in charged state, and unfavourable redox potentials. Hence, the development of new ROMs is needed to push the boundaries of organic RFBs.

Paraquat (also known as methyl viologen), a well-known herbicide, is presently among the best performing anolyte ROMs holding one or two negative charges in aqueous RFBs.[17, 22-23] Due to its general toxicity and the alleged neurotoxicity, however,

the paraquat has been banned both in the US and European Union and became superseded by the less toxic diquat family of the herbicides. Diquat herbicides act by inhibition of the electron transfer chain in photosystem I of the plants by interferentially accepting the transferred electrons, which consequently kill the plant leaves.[24] The role of diquat as an electron receiver, in which the 2,2'-bipyridylium ring moiety electrochemically generates radical cations (Scheme 1a), inspires its potential use as an anolyte material in RFBs. In the present study, a series of 2,2'-bipyridylium ROMs bearing different dialkylating functionalities have been constructed to investigate the structural effects on the electrochemical properties and stability. The degradation mechanisms of the radical cations have been elucidated leading to the design of stable diquat molecules. When coupled with an established catholyte material, (ferrocenylmethyl)trimethylammonium chloride (FcNCl),[16] the diquat molecules have formed aqueous RFBs with the cell voltages of around 1.1 V that also have produced great stability over long cycling tests, demonstrating the combined characteristics favoured for RFB anolyte materials.

The molecular structures of the 2,2'-bipyridylium series are shown in Scheme 1b. Except the progenitor of this class, the dimethyl 2,2'-dipyridyl (**1**), the other four derivatives feature an ethylene linker bridging the two adjacent nitrogen centers to form a third heterocyclic ring fused with the bipyridyl backbone. The synthesis is straightforward via one-step substitution reaction with quantitative yields (Scheme 1c).

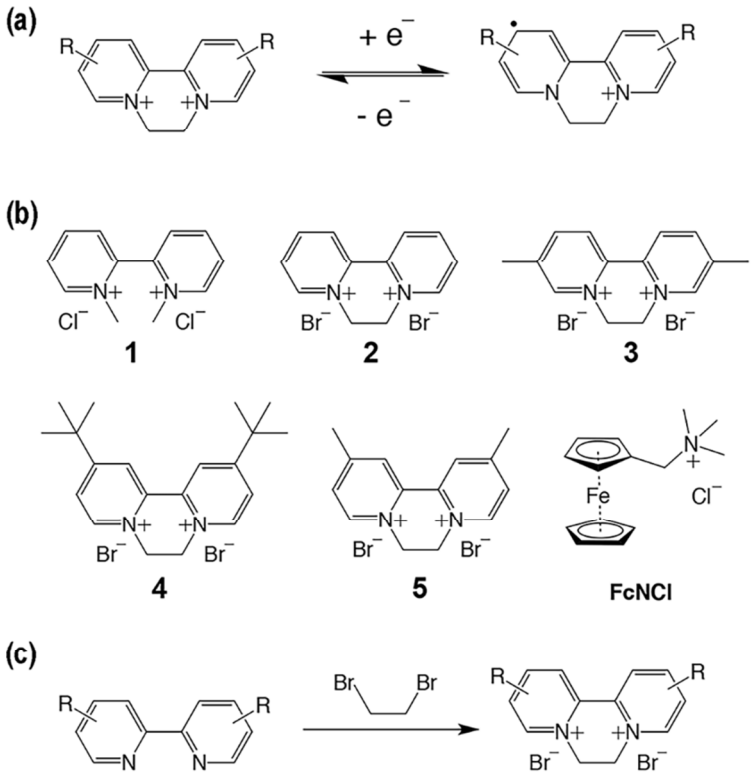

Scheme 1. (a) Electrochemical reactions of diquat compounds; (b) molecular structures of the diquat anolytes (**1**-**5**) and FcNCl catholyte; (c) general synthetic approach.

The chemical stability of ROMs is of fundamental importance for achieving good electrochemical cyclability.[25] The structural feature of ethylene linking in the diquat ROMs has been demonstrated to significantly affect their stability. The electrochemical reduction of the progenitor **1** to $\mathbf{1}^{+\bullet}$ is completely irreversible at neutral pH, as seen from the cyclic voltammograms (CVs) shown in Figure 1a, indicating the occurrence of continuous parasitic side reactions. Moreover, **1** has poor solubility in aqueous solutions. On the contrary, diquats **2** to **5** have more favorable properties as anolyte materials for RFBs. First, the solubilities of diquats **2**-**5** are 2.2 M, 2.6 M, 1.7 M, and 2.7 M, respectively, in aqueous electrolytes, promising for achieving high energy density. Second, they can be reversibly reduced under the same conditions as **1**, indicated by the near-identical 200 repeated CV curves (Figure 1b).

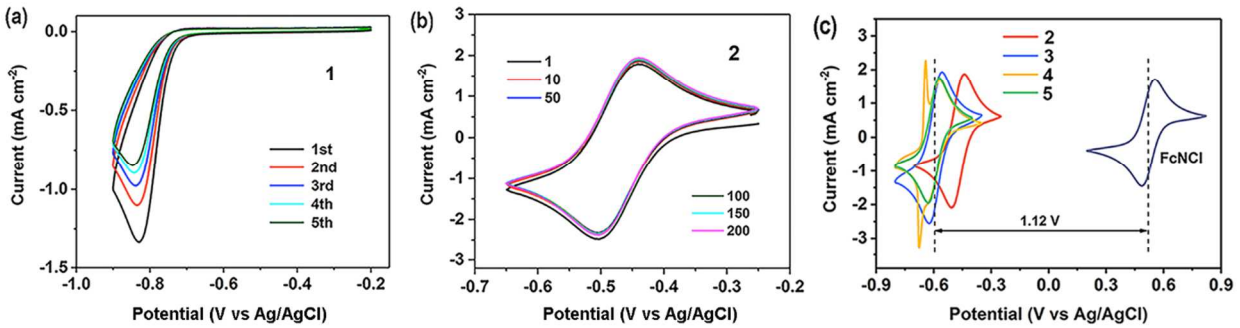

Figure 1. CV scans of 10 mM ROM in 1 M NaCl: (a) 5 cycles of **1**, (b) 200 cycles of **2**, and (c) Diquat **2-5** and FcNCl.

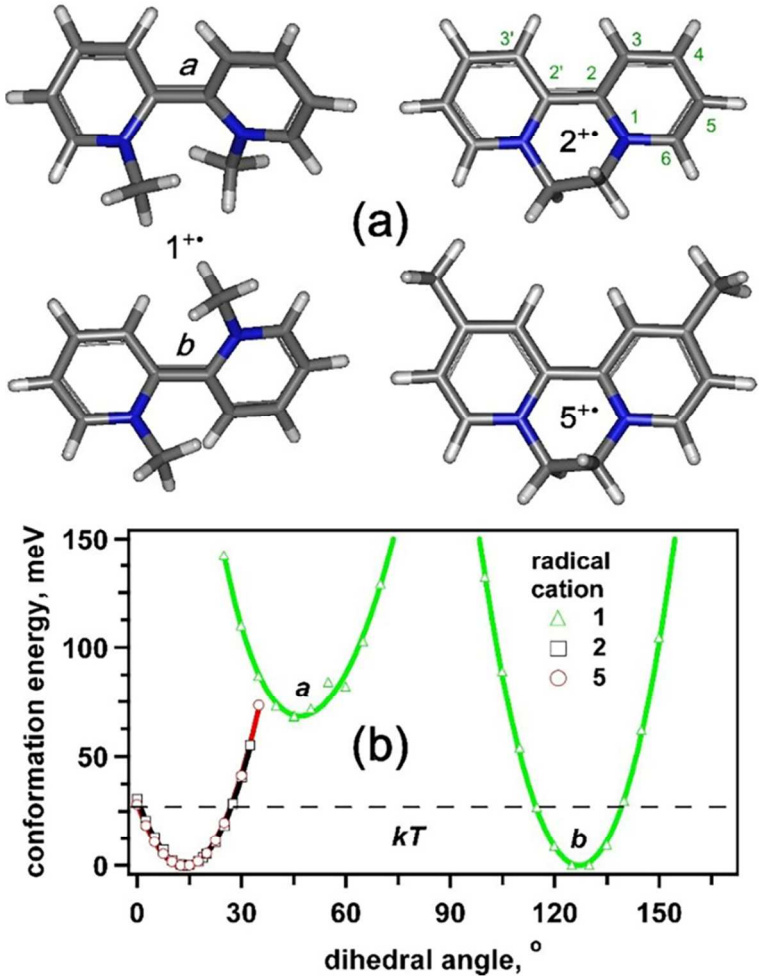

Figure 2. (a) Geometry-optimized hydrated $\mathbf{1}^{+\bullet}$ (conformers *a* and *b*), $\mathbf{2}^{+\bullet}$, and $\mathbf{5}^{+\bullet}$ (with atoms in the pyridyl rings numbered on the right) and (b) conformation energies of these radical cations plotted vs. dihedral angle ϕ between the two pyridyl rings (*symbols*). The dashed horizontal line indicates the thermal energy *kT* at 300 K. The inversion barriers for $\mathbf{2}^{+\bullet}$ and $\mathbf{5}^{+\bullet}$ are close to *kT*, so these radical cations readily flex in solution.

To understand the degradation mechanisms, density functional theory (DFT) calculations were used to investigate the molecular configurations of the 2,2'-bipyridylium radical cations. Due to the proximity of two *N*-methyl groups, the unbridged $\mathbf{1}^{+\bullet}$ lacks stabilization through π-conjugation (Table 1 and Figure 2). In the lowest energy conformers of $\mathbf{1}^{+\bullet}$, the two pyridyl rings form angles ϕ of ~45° or ~128° with each other. In contrast, for the diquat radical cations ($\mathbf{R}^{+\bullet}$), this angle is only ≈14° in the lowest energy conformer. However, the potential surface is shallow, and the inversion barrier (25-30 meV) is close to the thermal energy,[26] so $\mathbf{R}^{+\bullet}$ is structurally flexible in solution (Section S3.1.2). This dynamic flattening leads to improved π-conjugation over the two pyridyl rings in $\mathbf{R}^{+\bullet}$, which also increases the one-electron redox potential of the diquats relative to **1** (Table 1). This change has significant implications for the stability of $\mathbf{R}^{+\bullet}$ in aqueous solutions.

Inspired by previous kinetic studies,[27-29] the chemical stability of the diquat radical cations is closely associated with a proton catalyzed disproportionation reaction of two $\mathbf{R}^{+\bullet}$ species to $\mathbf{R}^{0}$ and $\mathbf{R}^{2+}$ (reaction 1 in Table 1).[30] This reaction is strongly endergonic, judged by $\Delta G^{o}(1)>0$ in Table 1. But in an aqueous solution, $\mathbf{R}^{0}$ (which is a strong base) becomes protonated to $\mathbf{R}H^{+}$ (reaction 2), leading to the overall exergonic reaction 1+2 under the standard conditions (Table 1 and Section S3.1.4). Accordingly, the second order decay of $\mathbf{R}^{+\bullet}$ is rapid at low pH, but is very slow at neutral and high pH because the overall reaction becomes endergonic with suppressed reaction 2. The driving force of reaction 1 is the difference in the redox potentials for the $\mathbf{R}^{2+}/\mathbf{R}^{+\bullet}$ and $\mathbf{R}^{+\bullet}/\mathbf{R}^{0}$ redox couples (Table 1). Consequently, **1** (which has the lowest estimated redox potential) has the lowest driving force for overall reaction 1+2 and, according to our estimates in Table 1, this reaction becomes favorable even at pH 7. On these grounds, $\mathbf{2}^{+\bullet}$, $\mathbf{3}^{+\bullet}$ and $\mathbf{5}^{+\bullet}$ are comparably stable and also are much more stable than $\mathbf{1}^{+\bullet}$ in neutral aqueous solutions.

Table 1. Redox potentials, reaction free energies, and other relevant properties for **1**-**5**.

R	$E_{1/2}$ (exp.) V vs Ag/AgCl	E^o, (calc.) V vs Ag/AgCl		ΔG^0(1), disp., eV	ΔG^0(2), prot., eV	ΔG^0(1+2), total, eV	ΔG(1+2), *pH*=7, eV	C_3-C_2-$C_{2'}$-$C_{3'}$ dihedral angle ϕ, °		
	1st	1st	2nd					R^{2+}	$R^{+\bullet}$	R^0
1	-	-0.65	-1.32	0.67	-1.24	-0.57	-0.16	89.4	127.6	149.3
2	-0.474	-0.29	-1.27	0.98	-0.91	0.07	+0.48	23.3	13.9	5.0
3	-0.589	-0.45	-1.40	0.95	-1.15	-0.20	+0.21	22.5	13.7	5.4
4	-0.600	-0.51	-1.29	0.78	-1.03	-0.25	+0.16	22.4	14.3	3.9
5	-0.600	-0.46	-1.38	0.92	-1.03	-0.11	+0.30	23.5	13.2	4.2
MV[b]	-0.532	-0.23	-1.40	1.18	-0.78	0.40	+0.81	90.0	2.1	0.4

$\Delta G^0(1)$, $\Delta G^0(2)$, and $\Delta G^0(1+2)$ are the computed standard free energies for the radical disproportionation $2\mathbf{R}^{+\bullet} \rightarrow \mathbf{R}^{2+} + \mathbf{R}^0$ (***reaction 1***), the protonation of $\mathbf{R}^0$ (***reaction 2***); and the overall reaction.

To further demonstrate the chemical stability of the diquat radical cations at pH 7, continuous wave electron paramagnetic resonance (EPR) was used to investigate the radical characteristics. The sample was prepared by electrochemically charging 10 mM **5** in a **5**/FcNCl flow cell (Figure S4). To establish the identity of paramagnetic species, the $\mathbf{5}^{+\bullet}$ anolyte solution was diluted 1:10 v/v to reduce resonance line broadening due to degenerate electron and spin exchange so that the EPR spectrum can be resolved (Figure 3a). The hyperfine coupling constants (hfcc's) in ^{1}H and ^{14}N nuclei were compared with the ones computed by using our models (Section S3.1.3) and previously reported.[26, 31-32] The results established $\mathbf{5}^{+\bullet}$ as the sole progenitor of this EPR spectrum. Our computed values for $\mathbf{5}^{+\bullet}$ (Table S2) correspond well to experimental estimates obtained assuming dynamic averaging of the pseudoequatorial and pseudoaxial methylene protons in the radical cations,[26] conclusively proving the DFT-predicted structural flexibility of the radical cations in solution. Figure 3b shows the first-derivative EPR spectrum of 10 mM $\mathbf{5}^{\bullet+}$ (which appears as an unresolved, exchange-broadened singlet at this concentration) and the decay of the doubly integrated EPR signal (which is proportional to the

concentration of the paramagnetic species) over time. The decay is because the radical cation slowly degrades in the solution via the proton-assisted disproportionation (see above). Second order extrapolation of these kinetics gives the half-decay life time $t_{1/2}$ of 250 h, suggesting excellent calendar life stability of $\mathbf{5}^{\bullet+}$ in the unbuffered aqueous electrolyte.

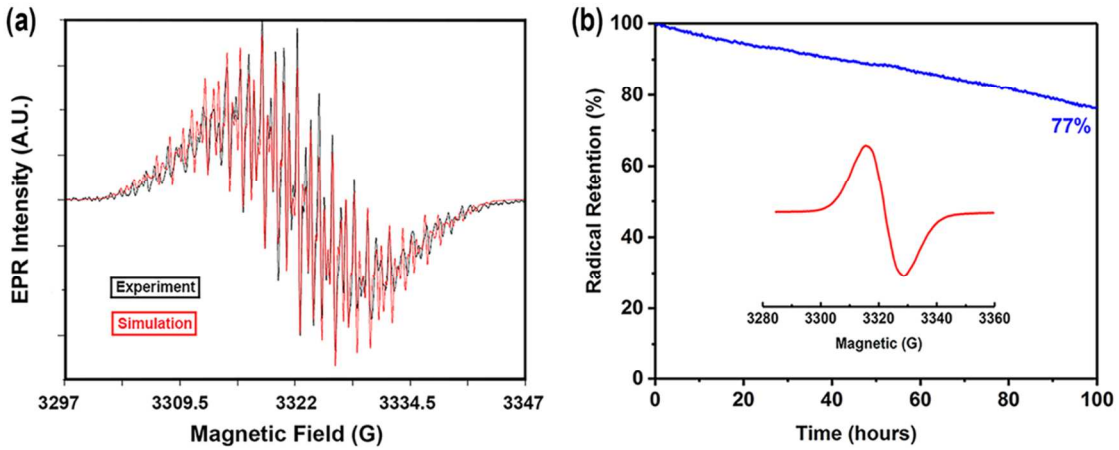

Figure 3. (a) Experimental and simulated first-derivative continuous-wave EPR spectra of electrochemically generated 1 mM $5^{+\bullet}$ in 1 M NaCl solution (X-band, 0.1 G modulation at 100 kHz). Due to rapid degenerate electron exchange[32-33] some resonance lines in the wings are selectively broadened and shifted, which was not taken into account in our EPR simulation. Dynamic averaging of the methylene hfcc's was assumed. (b) The first derivative X-band EPR spectrum *(inset)* and decay kinetics of the doubly integrated EPR signal observed in electrochemically generated 10 mM $5^{+\bullet}$ in 1 M NaCl.

Substitution with the electron donating groups lowers the redox potentials of ROMs, increasing the cell voltage and energy density.[19] Figure 1c shows the CV curves of **2-5** as well as **FcNCl** (also see Table S1). As a substituent-free derivative, **2** has a redox potential of -0.474 V vs Ag/AgCl. The alkyl groups on the aromatic rings negatively shift the redox potential because of the electron-donating effect, leading to lower potentials of -0.589 V for **3** and of -0.600 V for **4** and **5**. Excellent electrochemical reversibility was observed for all of these diquats as suggested by the near unity peak current ratios and the identical redox peak positions in the CV profiles obtained at all scan rates (see Table S1 and Figure S3a). Diquat **5** has been selected for

further scrutiny because of the lowest redox potential, the best solubility, and the high stability of its radical cation. In addition, the redox potential of **5** is even lower than that of the reported paraquat (methyl viologen)[17] in the same neutral electrolyte (Figure S1b). When coupling **5** to FcNCl, a RFB with a theoretical cell voltage of 1.12 V can be obtained. To investigate the electrochemical kinetics of **5**, linear sweep voltammetry (LSV) was performed using a glassy carbon rotating disk electrode (Figure S2). Based on the LSV profiles, Koutecky–Levich analysis yielded a kinetic rate constant (k_0) of 6.4×10^{-3} cm/s for the one-electron reduction of **5** (see Section S3.2).[6, 34] This rate of interfacial electron transfer is considerably faster than the estimates obtained for metal ion compounds in aqueous RFBs;[6] and this trait is favored for achieving high efficiency. Although not relevant for RFBs since the electrolyte flows facilitate convection-based mass transport, the diffusion coefficient of **5** could still be obtained from both CV and LSV measurements (see S3.3 and Figure S3).

Encouraged by the above results, the galvanometric cycling performance of **5**/FcNCl flow cells was examined. Because both of the ROMs are cations, an anion exchange membrane (Selemion^{TM} AMV) was used to minimize their crossover. The **5**/FcNCl flow cell containing 10 mM each of the two ROMs in 1 M NaCl solution was tested over 1,000 charge/discharge cycles at a current density of 5 mA/cm^2 (Figure 4a). One-electron reactions were indicated by the single potential plateau in the voltage-capacity plots (inset). A single charge/discharge cycle took 5.5 min, so the overall duration of the test (92 h) was equivalent to ~ 0.4 $t_{1/2}$. This flow cell demonstrated the mean Coulombic efficiency (CE) exceeding 99.96%, the voltage efficiency (VE) of 93.3%, and the energy efficiency (EE) of >93.3% with the material utilization ratio of 85%. It also exhibited remarkable cycling stability with the mean capacity fade of 0.016% per cycle throughout the entire cycling test.

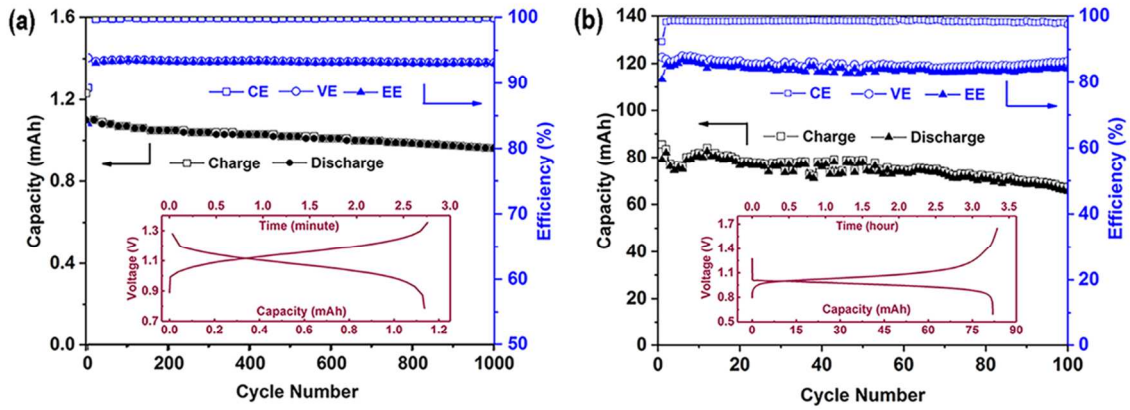

Figure 4. The cycling efficiencies, capacities, and voltage-capacity dependencies for flow cells operated at 5 mA cm^{-2}: (a) 10 mM ROMs in 1 M NaCl; and (b) 0.5 M ROMs in 1.5 M NaCl.

Flow cell testing with concentrated ROM solutions is always more challenging. The test result for a **5**/FcNCl flow cell containing 0.5 M ROMs are shown in Figure 4b. A complete cycle took 6.6 h, and this 100-cycle test took 597 h. Good cell efficiencies were still observed, with an average CE of 98.4%, VE of 85.5%, and EE of 84.1%. The capacity fade was 0.2% per cycle, but the material utilization ratio was lower than in the low concentration regime (62% vs 83%). Post mortem examination indicated solid deposits on the graphite felt electrode at the anolyte side, suggesting a possible oversaturation of $5^{+\bullet}$ near the electrodes during the reduction of **5**. The formation of solid deposits would qualitatively explains the reduced material utilization, slow capacity fading, and "bumpy" capacity profile in Figure 4b. Compared with the reported methyl viologen anolyte tested at the same 0.5 M concentration and with the same FcNCl catholyte,[16] the relatively inferior efficiency of the flow cell using **5** anolyte is primarily because of the low solubility of the $5^{+\bullet}$, while the cycling stability is difficult to judge due to the >10-fold slower charge rate used in this study. The result suggests further optimization of the diquat structure may be necessary to improve the solubility of $5^{+\bullet}$ to prevent precipitation and improve efficiency. However, even with these complications in the high-concentration regime, the

achieved cycling stability still places this redox system among the best performing aqueous RFBs.

In conclusion, we demonstrate that diquat dications are highly suitable as stable redox active materials to store negative charges in aqueous RFBs. These materials have low redox potentials and yield exceptionally stable radical cations in neutral aqueous solutions when reduced electrochemically, resulting in remarkable cycling performance in flow cells at moderate ROM concentrations. As a critical contribution, this work unveils the physical organic-based mechanistic origins of the high stability of the 2,2'-bipyridylium radical species, which indicates the high planar π-conjugation is key to achieving stable aromatic-based ROMs. Although additional molecular engineering may be still needed to further improve the chemical stability and solubility of the charged species, the diquat family anolytes have demonstrated great potential in harvesting stable, sustainable stationary storage of renewable energy. The fundamental insights gained from the stability study also suggest a promising direction to increase the long cyclability and advance the technical progress of organic RFBs.

ASSOCIATED CONTENT

Supporting Information.

The Supporting Information is available free of charge on the ACS Publication website, including details experimental methods; synthesis and characterizations of **1**-**5** and FcNCl; DFT calculations of redox potential, conformational energy, EPR parameters, and reaction energetics; LSV curves and analysis; supplemental CV curves and analysis.

AUTHOR INFORMATION

Corresponding Authors

* Email: xwei18@iupui.edu (X.W.)

* Email: zzhang@anl.gov (Z. Z.)

Author Contributions

§ J. H. and Z. Y. contributed equally to this work.

Notes

The authors declare no competing financial interest.

ACKNOWLEDGMENT

This work was supported as part of the Joint Center for Energy Storage Research (JCESR), an Energy Innovation Hub funded by the U.S. Department of Energy (DOE). EPR measurement and DFT calculations were supported by the William R. Wiley Environmental Molecular Sciences Laboratory (EMSL) at Pacific Northwest National Laboratory (PNNL). The submitted manuscript has been created by UChicago Argonne, LLC, Operator of Argonne National Laboratory ("Argonne"). Argonne, a U.S. Department of Energy Office of Science laboratory, is operated under Contract No. DE-AC02-06CH11357. Prof. X. Wei also thanks Indiana University-Purdue University Indianapolis (IUPUI) for providing the start-up fund to write the manuscript.

REFERENCES

(1) Dunn, B.; Kamath, H.; Tarascon, J. M., Electrical Energy Storage for the Grid: A Battery of Choices. *Science* **2011,** *334* (6058), 928-935.
(2) Wang, W.; Luo, Q.; Li, B.; Wei, X.; Li, L.; Yang, Z. G., Recent Progress in Redox Flow Battery Research and Development. *Adv. Funct. Mater.* **2013,** *23* (8), 970-986.
(3) Noack, J.; Roznyatovskaya, N.; Herr, T.; Fischer, P., The Chemistry of Redox-Flow Batteries. *Angew. Chem. Int. Edit.* **2015,** *54* (34), 9775-9808.
(4) Soloveichik, G. L., Flow Batteries: Current Status and Trends. *Chem. Rev.* **2015,** *115* (20), 11533-11558.
(5) Skyllas-Kazacos, M.; Chakrabarti, M. H.; Hajimolana, S. A.; Mjalli, F. S.; Saleem, M., Progress in Flow Battery Research and Development. *J. Electrochem. Soc.* **2011,** *158* (8), R55-R79.
(6) Weber, A. Z.; Mench, M. M.; Meyers, J. P.; Ross, P. N.; Gostick, J. T.; Liu, Q., Redox Flow Batteries: A Review. *J. Appl. Electrochem.* **2011,** *41* (10), 1137-1164.
(7) Leung, P.; Shah, A. A.; Sanz, L.; Flox, C.; Morante, J. R.; Xu, Q.; Mohamed, M. R.; Ponce de Leon, C.; Walsh, F. C., Recent Developments in Organic Redox Flow Batteries: A Critical Review. *J. Power Sources* **2017,** *360*, 243–283.
(8) Park, M.; Ryu, J.; Wang, W.; Cho, J., Material Design and Engineering of Next-Generation Flow-Battery Technologies. *Nat. Rev. Mater.* **2017,** *2* (1), Article 16080.
(9) Wei, X.; Pan, W.; Duan, W.; Hollas, A.; Yang, Z.; Li, B.; Nie, Z.; Liu, J.; Reed, D.; Wang, W.; *et al.*, Materials and Systems for Organic Redox Flow Batteries: Status and Challenges. *ACS Energy Lett.* **2017,** *2* (9), 2187-2204.
(10) Winsberg, J.; Hagemann, T.; Janoschka, T.; Hager, M. D.; Schubert, U. S., Redox-Flow Batteries: From Metals to Organic Redox-Active Materials. *Angew. Chem. Int. Edit.* **2017,** *56*, 686 –711.
(11) Ding, Y.; Zhang, C.; Zhang, L.; Zhou, Y..; Yu, G., Molecular Engineering of Organic Electroactive Materials for Redox Flow Batteries. *Chem. Soc. Rev.* **2018,** *47* (1), 69-103.
(12) Huskinson, B.; Marshak, M. P.; Suh, C.; Er, S.; Gerhardt, M. R.; Galvin, C. J.; Chen, X.; Aspuru-Guzik, A.; Gordon, R. G.; *et al.*, A Metal-Free Organic-Inorganic Aqueous Flow Battery. *Nature* **2014,** *505* (7482), 195-198.
(13) Yang, B.; Hoober-Burkhardt, L.; Wang, F.; Prakash, G. K. S.; Narayanan, S. R., An Inexpensive Aqueous Flow Battery for Large-Scale Electrical Energy Storage Based on Water-Soluble Organic Redox Couples. *J. Electrochem. Soc.* **2014,** *161* (9), A1371-A1380.
(14) Lin, K.; Chen, Q.; Gerhardt, M. R.; Tong, L.; Kim, S. B.; Eisenach, L.; Valle, A. W.; Hardee, D.; Gordon, R. G.; Aziz, M. J.; *et al.*, Alkaline Quinone Flow Battery. *Science* **2015,** *349* (6255), 1529-1532.
(15) Janoschka, T.; Martin, N.; Hager, M. D.; Schubert, U. S., An Aqueous Redox-Flow Battery with High Capacity and Power: The TEMPTMA/MV System. *Angew. Chem. Int. Edit.* **2016,** *55* (46), 14425-14428.
(16) Hu, B.; DeBruler, C.; Rhodes, Z.; Liu, T., Long-Cycling Aqueous Organic Redox Flow Battery (AORFB) toward Sustainable and Safe Energy Storage. *J. Am. Chem. Soc.* **2017,** *139* (3), 1207-1214.
(17) Liu, T.; Wei, X.; Nie, Z.; Sprenkle, V.; Wang, W., A Total Organic Aqueous Redox Flow Battery Employing a Low Cost and Sustainable Methyl Viologen Anolyte and 4-HO-TEMPO Catholyte. *Adv. Energy Mater.* **2016,** *6* (3), 1501449.
(18) Orita, A.; Verde, M. G.; Sakai, M.; Meng, Y. S., A Biomimetic Redox Flow Battery Based on Flavin Mononucleotide. *Nat. Commun.* **2016,** *7*, Article Number 13230.

(19) Lin, K.; Gomez-Bombarelli, R.; Beh, E. S.; Tong, L.; Chen, Q.; Valle, A.; Aspuru-Guzik, A.; Aziz, M. J.; Gordon, R. G., A Redox-Flow Battery with An Alloxazine-Based Organic Electrolyte. *Nat. Energy* **2016,** *1*, Article 16102.
(20) Hollas, A.; Wei, X.; Murugesan, V.; Nie, Z.; Li, B.; Reed, D.; Liu, J.; Sprenkle, V.; Wang, W., A Biomimetic High-Capacity Phenazine-Based Anolyte for Aqueous Organic Redox Flow Batteries. *Nat. Energy* **2018,** *3* (6), 508-514.
(21) DeBruler, C.; Hu, B.; Moss, J.; Luo, J.; Liu, T., A Sulfonate-Functionalized Viologen Enabling Neutral Cation Exchange, Aqueous Organic Redox Flow Batteries toward Renewable Energy Storage. *ACS Energy Lett.* **2018,** *3* (3), 663-668.
(22) DeBruler, C.; Hu, B.; Moss, J.; Liu, X.; Luo, J.; Sun, Y.; Liu, T., Designer Two-Electron Storage Viologen Anolyte Materials for Neutral Aqueous Organic Redox Flow Batteries. *Chem* **2017,** *3* (6), 961-978.
(23) Beh, E. S.; De Porcellinis, D.; Gracia, R. L.; Xia, K.; Gordon, R. G.; Aziz, M. J., A Neutral pH Aqueous Organic-Organometallic Redox Flow Battery with Extremely High Capacity Retention. *ACS Energy Lett.* **2017,** *2* (3), 639-644.
(24) Fuerst, E. P.; Norman, M. A., Interactions of Herbicides with Photosynthetic Electron Transport. *Weed Sci.* **1991,** *39*, 458-464.
(25) Wei, X.; Xu, W.; Huang, J.; Zhang, L.; Walter, E.; Lawrence , C.; Vijayakumar, M.; Henderson, W. A.; Liu, T.; Cosimbescu, L.; *et al.*, Radical Compatibility with Nonaqueous Electrolytes and Its Impact on an All-Organic Redox Flow Battery. *Angew. Chem. Int. Edit.* **2015,** *54* (30), 8684-8687.
(26) Sullivan, P. D.; Williams, M. L., ESR and X-Ray Study of the Structure of Diquat (6,7-Dihydrodipyrido[1 ,2-a:2'1,' -c]pyrazinediium) Cation Radical and Dication. *J. Am. Chem. Soc.* **1976,** *98*, 1711-1716.
(27) Solar, S.; Solar, W.; Getoff, N.; Holcman, J.; Sehested, K., Hydrogen-atom Attack on Methyl Viologen in Aqueous Solution Studied by Pulse Radiolysis. *J. Chem. Soc. Faraday Trans. 1* **1984**, 2929-2934.
(28) Solar, S.; Solar, W.; Getoff, N.; Holcman, J.; Sehested, K., Pulse Radiolysis of Methyl Viologen in Aqueous Solutions. *J. Chem. Soc., Faraday Trans. 1* **1982,** *78*, 2467-2477.
(29) Venturi, M.; Mulazzani, Q. G.; Hoffman, M. Z., Radiolytically-Induced One-Electron Reduction of Methyl Viologen in Aqueous Solution: Stability of the Radical Cation in Acidic and Highly Alkaline Media. *Radiat. Phys. Chem.* **1984,** *23*, 229-236.
(30) Hu, B.; Tang, Y.; Luo, J.; Grove, G.; Guo, Y.; Liu, T., Improved Radical Stability of Viologen Anolytes in Aqueous Organic Redox Flow Batteries. *Chem. Commun.* **2018,** *54* (50), 6871-6874.
(31) Sanchez-Palacios, A.; Delgardo, R., ESR Study of the Radical Cations 1,1'-Dimethylene and 1,1'-Trimethylene 2,2'-Bipyridinium: Charge-Transfer Complexes between their Dications and the Donor Cysteine. *Appl. Spectrosc.* **1994,** *48*, 926-932.
(32) Rieger, A. L.; Rieger, P. H., Magnetic Resonance Studies of Some Bipyridylium Dications and Cation Radicals. *J. Phys. Chem.* **1984,** *88*, 5845.
(33) Grampp, G.; Mladenova, B. Y.; Kattnig, D. R.; Landgraf, S., ESR and ENDOR Investigations of the Degenerate Electron Exchange Reactions of Various Viologens in Solution. Solvent Dynamical Effects. *Appl. Magn. Reson.* **2006,** *30*, 145-164.
(34) Bard, A. J.; Faulkner, L. R., *Electrochemical Methods: Fundamentals and Applications*. 2nd ed.; John Wiley & Sons Inc: New York, USA, 2000.

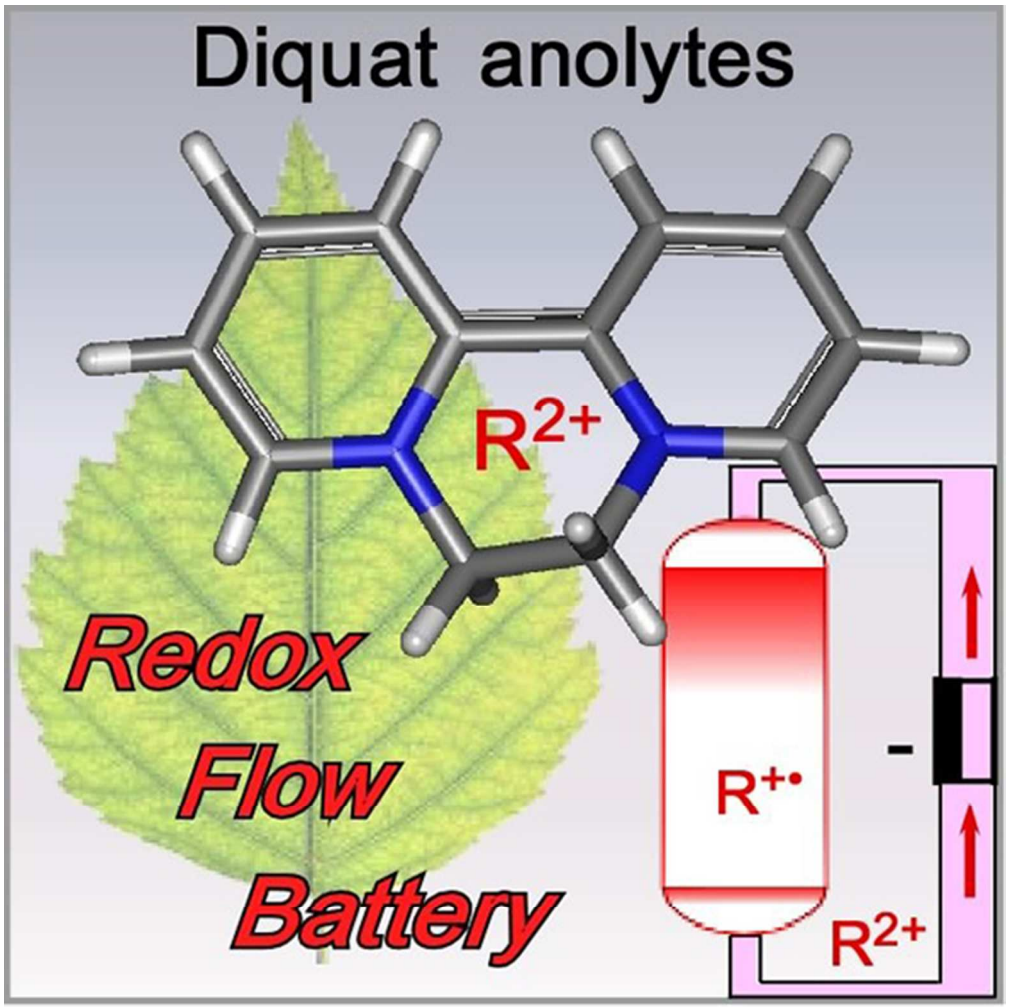

50x50mm (300 x 300 DPI)